Prediction of microstructure for heat treatment process in dual phase steels using Cellular Automata

K Vijay Reddy

Department of Metallurgical and Materials Engineering

National Institute of Technology Rourkela

Prediction of microstructure for heat treatment process in dual phase steels using Cellular Automata

Thesis submitted in partial fulfillment

of the requirements of the degree of

Master of Technology

in

Metallurgical and Materials Engineering

by

K Vijay Reddy

(Roll Number: 214MM1438)

Under the supervision of

Dr. S. Pal

May, 2016

Department of Metallurgical and Materials Engineering

National Institute of Technology Rourkela

Department of Metallurgical and Materials Engineering

National Institute of Technology Rourkela

May, 2016

Certificate of Examination

Roll Number: 214MM1438

Name: K Vijay Reddy

Title of Thesis: Prediction of microstructure for heat treatment process in dual phase steels using Cellular Automata

This is to certify that the thesis entitled, "**Prediction of microstructure for heat treatment process in dual phase steels using Cellular Automata**", submitted by **K Vijay Reddy** (Roll No: 214MM1438) is a record of an original and authentic research work carried out by him during 2015-2016 under my supervision and guidance in partial fulfillment of the requirements for the award of Master of Technology Degree in Metallurgical and Materials Engineering at the National Institute of Technology, Rourkela.

To the best of our knowledge, the matter embodied in the thesis has not been submitted to any other University/ Institute for the award of any degree.

_____

Dr. S. Pal
(pals@nitrkl.ac.in)
Assistant Professor
Department of Metallurgical and Materials Engineering
National Institute of Technology Rourkela

Acknowledgement

The work posed in this thesis is by far the most substantial attainment in my life and it would be unimaginable without people who affirmed me and believed in me. First and foremost I evince my profound reverence and deep regards to my guide Prof. S. Pal for exemplary guidance, supervising and constant encouragement throughout the course of this thesis. A gentleman embodied, in true form and spirit, I consider it to my good fortune to have consociated with him.

I would like to evince a deep sense of gratitude to estimable to Prof. S.K. Sarangi, Director and Prof. S. C. Mishra, Head of the Department of Metallurgical & Materials Engineering for providing us with best facilities and his timely suggestions.

I want to thank all other faculty members and staff of Department of Metallurgical & Materials Engineering for their constant support and encouragement during my research. My special thanks to Ph.D. scholar, Md. Meraj for his help, cooperation and encouragement. I would like to thank all my friends who made my journey at NIT Rourkela an indelible and gratifying experience.

Finally, my heartfelt gratitude towards my family for their tireless love and support throughout my life. They taught me the value of hard work by their own life example and the importance of truth and motivation in life. They gave me tremendous support during my stay in NIT Rourkela.

May, 2016 K Vijay Reddy

NIT Rourkela Roll Number: 214MM1438

Abstract

In this paper, a cellular automata method based model is proposed for simulating phase transformation kinetics of inter-critical heating of dual phase (DP) steel. This developed model deals with the kinetics of pearlite dissolution, ferrite transformation and austenite grain growth based on carbon diffusion process. Diffusion equation is discretized and solved by finite difference method (FDM) whereas austenite grain growth is controlled by transition rules applied in cellular automata algorithm. The model is operated in the temperature range of 730 ^{0}C to 890 ^{0}C for four different specimens of DP steel. This model predicts appropriately the microstructure and volume fraction of formed austenite during inter-critical heating of DP steel. In addition, this study shows that the presence of carbon and alloying elements enhances carbon equivalent of DP steel, helps in austenite formation.

Keywords: cellular automata; dual phase steel; inter-critical annealing; carbon equivalent.

Contents

List of figures

List of Tables

Chapter 1

Introduction

1.1 Heat treatment processes and microstructure prediction

Engineering materials need to have favorable properties based on the application such as strength, toughness, ductility, hardness, corrosion and wear resistance. These properties determines the quality of performance by that material. The properties in turn depends on the microstructure and hence study of evolution of microstructure becomes important. Microstructures are generally developed by heat treatment processes, mechanical processing and precipitation processes. Out of these, this work focuses on the heat treatment process. There are various heat treatment processes to change the morphology, for example annealing, tempering, normalizing, quenching etc. Depending on the heat treatment done on the steel, different microstructural phases can be obtained which alters the properties of the steel. For example, annealing is a process in which the steel is heated to a high temperature and then is cooled slowly. This process generally produces a refined microstructure and relieves stresses present in the microstructure. Whereas quenching is a rapid cooling process and produces a hard martensite phase in steels. Figure 1.1 illustrates the Continuous Cooling Transformation (CCT) phase diagram for steel and shows the effect of cooling rate on the final microstructure. It shows that as the cooling rate is decreased, coarser grains are formed with less residual stress

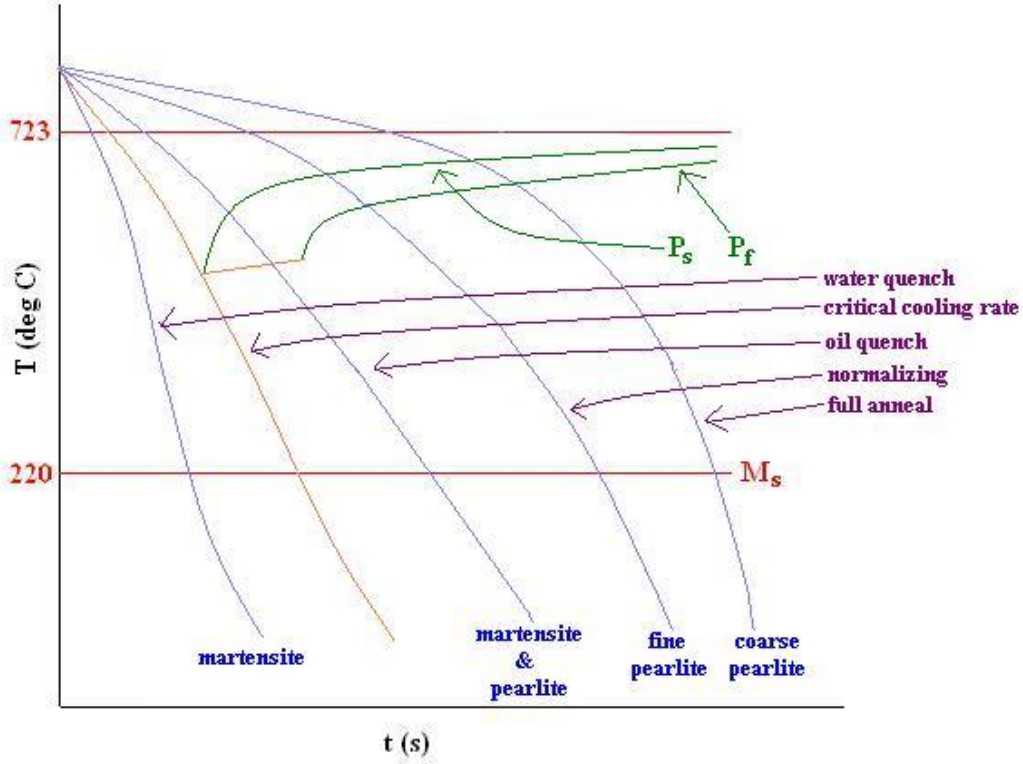

Figure 1.1: Continuous Cooling Transformation diagram for steel.

In the present work, evolution of microstructure during heat treatment process of dual phase (DP) steel is considered. Dual phase (DP) steels are a classification of advanced high strength steels (AHSS) consisting of a hard martensitic phase in the matrix of ferrite along with retained austenite or bainite (Al-Abbasi et al., 2003, Rashid et al., 1981, Sarwar and Priestner, 1996). DP steels are basically low carbon low alloy steels produced through inter-critical annealing followed by quenching process (Rocha et al., 2005). DP steels are highly beneficial for aerospace and automotive industries as they possess low weight/strength ratio, high tensile properties, enhanced formability and ductility (Allam and Abbas, 2015, Movahed et al., 2009, Hofmann et al., 2009, Matlock et al., 2012). These favorable properties are related to the microstructure morphology of dual phase steel where soft ferritic phase enhances ductility and hard martensitic phase increases strength. The microstructure morphology is dependent on the inter-critical heat treatment temperature

and process (Maleque et al., 2004). Inter-critical annealing heat treatment of DP steel is performed on recrystallized specimen as recrystallization process causes grain refinement, redistributes the carbide and releases residual stress in the specimen (Ahmad et al., 2014). Distribution and volume fraction of martensite present in quenched DP steel is strongly influenced by volume fraction of transformed austenite and its dispersion during heating of DP steel (Erdogan, 2003). Therefore, the austenite transformation during heating is significant in the development of the desired microstructure of DP steels although conventionally, much attention was given to the transformation and the effect of alloying elements during cooling of austenite into ferrite (Zhang et al., 2004, Pandi and Yue, 1994, Ricks et al., 1981, Cao et al., 2007). Austenite transformation depends on grain size; grain distribution, concentration of alloying element, heating process and inter-critical annealing temperature (Huang et al., 2004). Austenite stabilizers alloying elements (e.g. Ni, Mn, C) favors the transformation of austenite by decreasing the A_{c1} temperature whereas ferrite stabilizers (e.g. Cr, Mo) helps in the formation of ferrite by increasing the A_{c1} temperature (Schemmann et al., 2015, Girina et al., 2015). In addition, these alloying elements affect transformation rate, grain size, etc. during heating and also show significant impact on properties such as hardness, formability, and strength (Girina et al., 2015, Speich et al., 1981).

Experimental investigations on the variation in microstructure and properties of steel produced by different heat treatment processes have been reported in literature (Huang et al., 2004, Kim and Thomas, 1981). However, time constraints and research costs restrain the flexibility of conducting numerous and rigorous experimental analysis.

1.2 Simulation study of microstructure evolution

The microstructure evolution can also be numerically investigated using various modelling techniques. One of the simplest model is Avrami model which was initially developed by Kolmogorov and Avrami. This model functions on a set of equations and assumptions and describes the transformation mechanics of solid from one phase to another phase. However, conventional models based on Avrami type equations do not provide detail insight of mechanism related to the microstructure evaluation (Todinov, 2000). Hence to overcome

this limitation, various logic/rule based mesoscale microstructure modelling tools such as cellular automata, phase field modelling have been applied.

1.2.1 Phase Field Modelling

Phase field modelling is a very useful computational approach to develop the mesoscale based microstructure models. This approach uses a set of conserved and non-conserved variables which are also known as order parameters to define the morphology of the microstructure. One of the advantages of phase field modelling is that individual interface tracking is not required unlike sharp interface method. But during modelling, the thickness of the interface is adjustable which can sometimes be unrealistic. Other disadvantage of phase field modelling is that it can be modelled for only small domains as computational cost will increase drastically for larger domains. A better option is Cellular Automata (CA) method. Since Cellular Automata (CA) can handle large computational domains and capable of reducing the code complexity in terms of storage therefore, CA modelling has advantages over phase field modelling (Pietrzyk et al., 2015).

1.2.2 Cellular Automata Method

A cellular automaton is a collection of cells in the form of a one dimensional or two dimensional grid which store specific information in it termed as state variables. Cells in the grids can be of different patterns. Most commonly used grids are grids with square cells, hexagonal cells grid and triangular cells grid. Figure 1.2 shows an illustration of these three grid types.

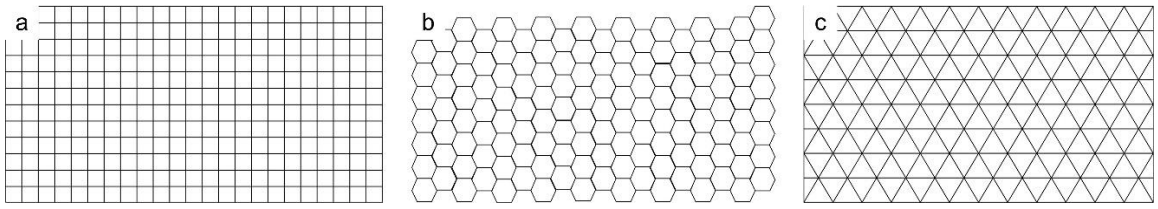

Figure 1.2: Types of cells in a grid: (a) Square grid, (b) hexagonal grid, (c) triangular grid

The matrix consisting of cells is represented by a set of color. Each cell having a unique state variable is represented by a unique color. This helps in representing the matrix in a pictorial form. The update of the values contained in the cells are obtained by implementing certain transition rules. The update of the cells also depends on the state of neighboring cells. Selection of the neighboring cells depends on the model. Either Von-Neumann neighborhood criteria can be chosen which consider four neighboring sites or Moore's Neighborhood criteria can be chosen which considers all the eight neighboring sites.

Microstructure evolution during heat treatment process can be modelled using CA method. Each phase is assigned with state variable and the evolution of the new phase will be updated with the time step. A large domain with multigrain microstructure can be analyzed using cellular automata model but the interface has to be tracked for the phases. In the next chapter, simulation models that have been developed so far showing the kinetics of phase transformation during continuous as well as inter-critical annealing processes, recrystallization are discussed.

Chapter 2

Microstructure Modelling

2.1 Johnson-Mehl-Avrami-Kolmogorov models

Manufacturing of dual phase (DP) steels is industrially a complex process. Unconventional thermal cycles during continuous annealing is one method to get dual phase steel. Simple models were developed to predict the microstructure evolution of dual phase steel during heat treatment process. One such model is intercritical annealing of a low-carbon steel for the production of industrial grade dual phase steel. This model is based on the Johnson-Mehl-Avrami-Kolmogorov (JMA) approach and the evolution of microstructure is predicted after recrystallization of ferrite model, evolution of austenite and decomposition model (Kulakov et al., 2014). Validation of models with the industrial or experimental data is also important. Pietrzyk et al. (2014) developed a model and validated it with the experimental analysis. Experiments included dilatometric tests and data of thermal cycle characteristics. The JMA approach can also be used to predict the austenization process in steels. Li et al., (2016) developed a numerical simulation based on the Johnson–Mehl–Avrami (JMA) equations. Different transformation kinetic parameters were obtained by thermo-mechanical simulator and austenite volume fraction and hardness were obtained and were validated using experiments.

2.2 Phase field modelling

Modelling using phase field techniques are also developed for the microstructure evolution during intercritical annealing. A two dimensional phase field model has been prepared of the cold rolled DP600 dual phase steel to describe the microstructure. Along with phase field model, a solute drag sub-model has also been integrated to study the effect of alloying elements on the mobility of interfaces. This model focuses on the relation between ferrite recrystallization and formation of austenite (Zhu et al., 2015). Another group of researchers used phase field method to simulate the quenching and partitioning in TRIP steel. The

carbon distribution in the microstructure during the heat treatment process was studied. The partitioning of the carbon from martensite to austenite was also investigated. The simulation was mainly based on the interface migration due to the difference in the free energy between martensite and austenite (Takahama et al., 2012).

2.3 Cellular Automata based modelling

Evolution of microstructure can be predicted using cellular automata modelling by describing the discrete spatial and temporal variables and by applying deterministic or probabilistic transition rules (Madej et al., 2013, Han et al., 2014, Mecozzi et al., 2011). Lin et al., (2016) developed a cellular automata model to predict the recrystallization process and microstructural evolution of Ni based super alloy. Cellular automata models has also been developed to study various processes during heat treatment of steel. Zhu et al., (2014) have prepared a two dimensional model to simulate the cooling process, recrystallization process, austenization and quenching process for a dual phase steel. The interface mobility and growth of phases due to the carbon diffusion has also been accurately predicted by the model. The morphology of microstructures obtained from the model is validated with the experiments. Another group of researchers have prepared a more realistic three dimensional CA model to study effect of the annealing process on the dual phase steel during heat treatment. This CA model, based on the grain boundary and interface velocity, predicts the growth of microstructure. In this model, the rate of cooling is also considered and subsequently the martensite phase formation is predicted (Bos et al., 2010). Numerous CA modelling based prediction of microstructures for cooling part of transformation of DP steel are available in literature. For example, Madej et al., (2013) developed a finite element and cellular automata multi-scale model for the static recrystallization of a two phase ferritic-pearlitic steel and Mecozzi et al., (2011) developed a three dimensional kinetic cellular automata model to predict the microstructural evolution during the annealing of a low alloy steel. These simulated models were also validated and were shown in good agreement with the experimental values. Han et al., (2016) used cellular automata method to simulate the microstructural evolution during the dynamic recrystallization process in an alloy steel. This simulation successfully predicts the relation between various parameters such as volume fraction, grain size and deformation temperature.

However, very few microstructure simulation has been developed using cellular automata method which shows the austenite transformation of a dual phase steel during heating to inter-critical temperatures (Halder et al., 2014). Moreover, the effect of alloying elements and carbon equivalent content has not been studied using the simulated models for the ferrite-pearlite to austenite transformation during inter-critical heating.

The objective of the present work is to develop a cellular automata model for predicting microstructure during the inter-critical heating of dual phase steel considering the phase transformation kinetics and study the effect of carbon equivalent on the austenite formation. The input microstructure in this model consists of ferrite and pearlite phases which are obtained from ferrite recrystallization model reported in literature (Zheng et al., 2013). Pearlite dissolution, ferrite transformation into austenite, and grain growth along with carbon diffusion is investigated in this paper. The developed model can be utilized as an initial microstructure for performing microstructure modelling for phase transformation during cooling.

Chapter 3

Cellular Automata Model

This chapter deals with the model description of transformation of ferrite and pearlite in dual phase steel into austenite during inter-critical heating. First, the kinetics of the process will be described. Initially, the microstructure consists of pearlite grains in the matrix of ferrite. Austenization process involves dissolution of pearlite grains and transformation of ferrite into austenite. The complete transformation process includes two major steps: austenite nucleation and growth (Reed-Hill and Abbaschian, 1973). Pearlite is a lamellar structure consisting of alternate layers of ferrite and cementite. The ferrite contains less than 0.025 wt. % of carbon and cementite contains 6.67 wt. % carbon. Steels with 0.77 wt. % carbon contains uniform pearlite grains and directly transforms into austenite at eutectoid carbon concentration. The main driving force for pearlite transformation into austenite is carbon diffusion process. Dissolution of pearlite phase is a very fast process because of short diffusion range, and is completed in a short span of time (Speich et al., 1981). Once pearlite grains are transformed to austenite, the carbon is redistributed and ferrite transformation occurs. Ferrite is a low carbon concentration phase and the initial transformation into austenite is a slower process than pearlite dissolution. Pearlite to austenite transformation starts when the temperature is just above A_{C1}, the ferrite to austenite transformation is prominently observed at higher temperatures. Ferrite is transformed into austenite when the ferrite carbon concentration reaches the equilibrium carbon concentration (i.e. AB line) at that temperature as shown in Figure 3.1. The equilibrium carbon concentration line and eutectoid composition (C_e) in Figure 3.1 may change their position according to the composition of the steel. Steels with higher concentration of Mn, Ni, and Cu will lower the A_{C1} line; increase the A_{C3} lines and the eutectoid temperature thereby widening the temperature range over which austenite is stable whereas elements such as Si, Cr, Al, and P increase the A_{C1} temperature and the eutectoid temperature, thus restricting the formation of austenite (Maalekian, 2007).

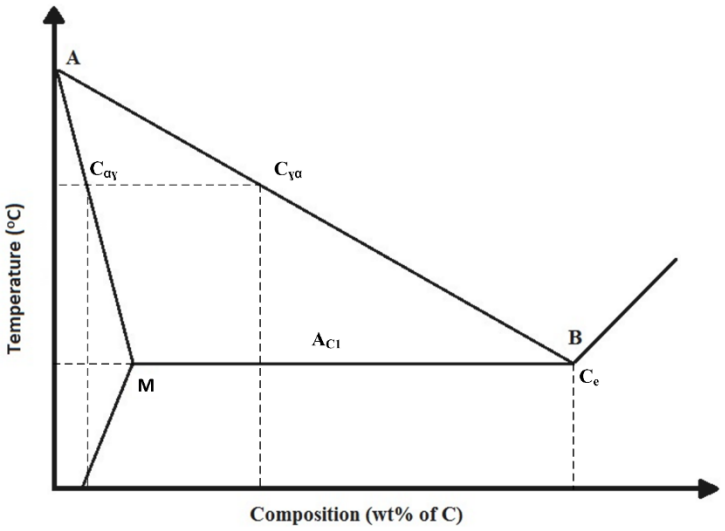

Figure 3.1: Fe-Fe3C diagram showing lower critical temperature line and upper critical temperature line for hypoeutectiod steels

In the present model, cellular automata (CA) method is applied to simulate the phase transformation of ferrite-pearlite phase into austenite phase during heating in dual phase (DP) steel and predict the microstructure after inter-critical heating. In addition to that, the effect of equivalent carbon content of DP steel on austenite formation is also investigated. But to simplify the understanding of carbon diffusion process, a single grain test model was developed and the diffusion process was visualized.

3.1 Single grain carbon diffusion model

The spatial system of the initial domain is discretized into two dimensional cells. The dimension of each cell is 1 µm and the total domain consists of (200 X 200) cells. The cells are assigned with state variables i.e. concentration value which provides the information regarding the carbon concentration in the cells. Initially, a high carbon concentration (0.7 wt. % carbon) is assigned at the center of the matrix and the remaining domain is considered to be zero concentration. The illustration is shown in figure 3.2.

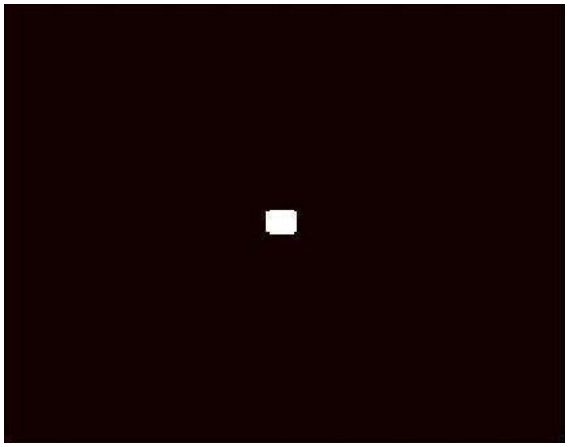

Figure 3.2: The CA matrix consisting of carbon concentration at the center of the domain.

3.1.1 Boundary Conditions

The size of the domain for the carbon diffusion process is restricted because of computational limits as computational time and cost will increase with increasing domain size. Therefore carbon diffusion process requires boundary conditions. In our model, symmetric boundary conditions are applied. The carbon diffusion takes place considering the neighborhood cells.

Two types of neighborhood cells can be considered:

1. Von-Neumann Neighborhood condition: In this neighborhood condition, four cells in the surrounding of the central cell is considered.
2. Moore's Neighborhood condition: In this neighborhood condition, eight cells around the central cell is considered.

Both neighborhood conditions are illustrated in figure 3.3. In this model, Von-Neumann neighborhood conditions are considered during the carbon diffusion process.

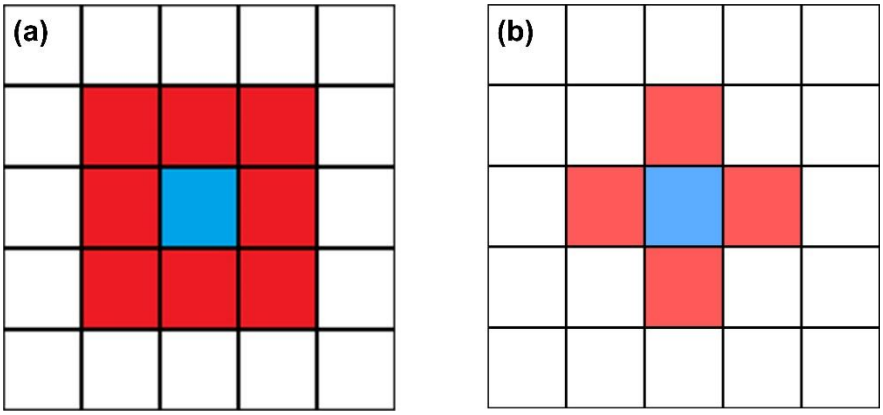

Figure 3.3: Illustration of the neighborhood conditions: (a) Moore's neighborhood, (b) Von-Neumann neighborhood.

3.1.2 Diffusion process

Diffusion process for in the domain is calculated by using discretized Fick's second law. Fick's second law is given by:

$$\frac{\partial C_\Psi}{\partial t} = D_\Psi \nabla^2 C_\Psi$$

where t is the time, C_Ψ is the concentration of solute, D_Ψ is the diffusion coefficient.

The discretized form is:

$$C_{i,j}^{t} = \frac{D_\Psi \Delta t}{\Delta_{xy}^2}\left(C_{i-1,j}^{t-1} + C_{i+1,j}^{t-1} + C_{i,j-1}^{t-1} + C_{i.j+1}^{t-1} + 4\,C_{i,j}^{t-1}\right) + C_{i,j}^{t-1} \qquad \textbf{Equation (1)}$$

where t is the time step, Δ_{xy} is dimension of one computational cell, i is the computational domain row and j is the computational domain column, $C_{i-1,j}^{t-1}$ is the cell on the left of the computed cell in the previous time step, $C_{i+1,j}^{t-1}$ is the cell on the right of the computed cell in the previous time step, $C_{i.j+1}^{t-1}$ is the cell above the computed cell in the previous time step, $C_{i,j}^{t-1}$ is the cell below the computed cell in the previous time step.

Δt is the condition of stability and is given by:

$$\Delta t \leq \frac{\Delta_{xy}^2}{4\,D_\Psi} \qquad \textbf{Equation (2)}$$

The cells containing higher carbon concentration starts diffusing to the lower concentration depending on the diffusion coefficient. The rate of carbon diffusion also depends on the temperature as diffusion process is faster at higher temperatures. **Figure 3.4** shows the diffusion process of the single grain.

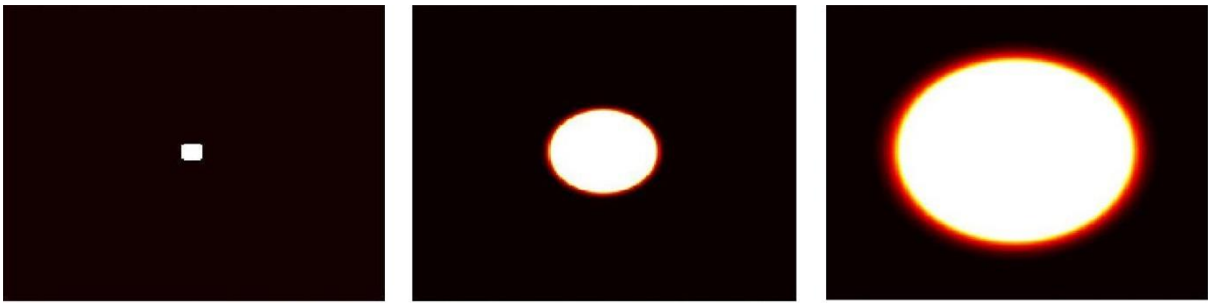

Figure 3.4*:* Illustration of diffusion process for a single grain in the computational domain.

To show the effect of boundary condition pictorially, the concentration grain is shifted to one side of the domain and then the code is run. Figure 3.5 shows that there is continuity in the domain and periodic boundary condition

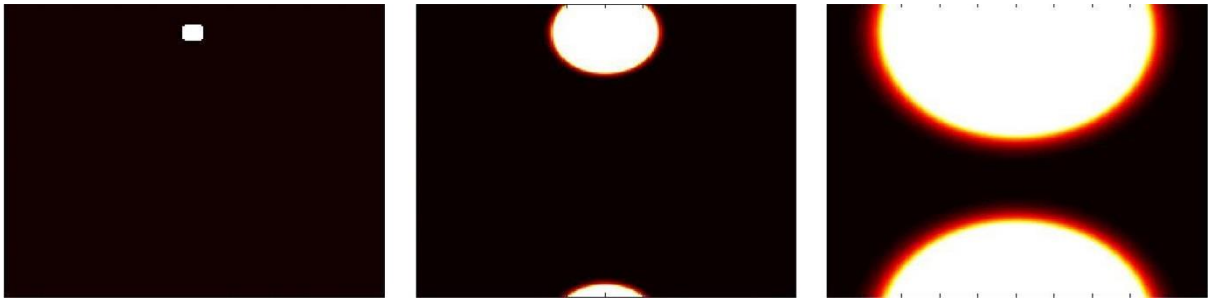

Figure 3.5: Effect of the periodic boundary condition on the diffusion process.

3.2 Multi grain model

In this model, a larger domain with multiple grains is considered. A dual phase steel microstructure is taken from the literature and is digitized for the heat treatment process simulation. The digitized image consists matrix of ferrite and pearlite grains. The dimension of each cell is 1 μm and the total domain consists of (147 X 495) cells. Representation of phases is the computational domain is done by assigning state variables for ferrite, pearlite and austenite. In the model, ferrite is assigned with 0 (zero), pearlite is assigned with 2,

austenite is assigned with 3, and grain boundary is assigned with 1 as the state variable. Carbon concentration and orientation of grains are assigned as internal variables. The ferrite and pearlite carbon concentrations are initialized to be 0.002 wt. % carbon and 0.7 wt. % carbon. Figure 3.6 shows the initial microstructure of dual phase steel as an input for the simulation. The kinetics of phase transformation is obtained by updating the variables according to the transition rules and heating rate. Transition rules are applied in this model for austenite nucleation and growth during the heating process.

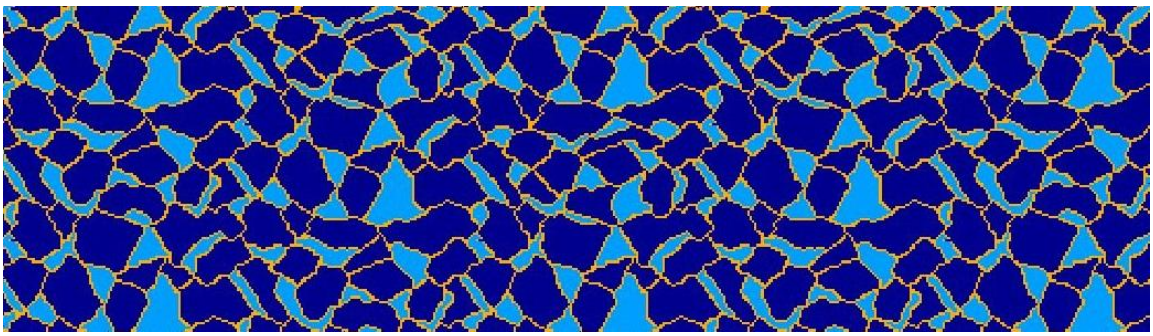

Figure 3.6: Initial microstructure as input for the simulation. (light blue- Pearlite, dark blue- Ferrite, yellow- Grain boundary).

3.2.1 Dual Phase steel composition

In this model, four different compositions of dual phase steel are considered and their compositions along with the carbon equivalent content are presented in Table 1. The volume fraction of ferrite and pearlite is calculated according to the weighted average of the carbon concentration of the DP steel specimen. The concentration of alloying element is varied to study their combined effect on the formation of austenite. The carbon equivalent (CE) content is calculated using Dearden and O'Neill equation (Kasuya et al., 1993):

$$CE = C + \frac{P}{2} + \frac{Mn}{6} + \frac{Mo}{4} + \frac{(Cr+V)}{5} + \frac{Ni}{15} \qquad \textbf{Equation (3)}$$

where C- wt. % of carbon concentration, P- wt. % of phosphorous, Mn- wt. % of manganese, Mo- wt. % of molybdenum, Cr- wt. % of chromium, V- wt. % of vanadium, and Ni- wt. % of nickel in the steel.

Specimens	C	Mn	Si	P	S	Cr	Mo	V	Al	Cu	Ni	Carbon Equivalent
Specimen 1	0.13	1.5	0.10	0.011	0.011	0.23	0.005	0.005	0.026	0.02	0.02	0.318
Specimen 2	0.081	1.12	0.35	0.008	0.008	0.52	-	-	-	0.38	0.31	0.396
Specimen 3	0.11	0.53	0.07	0.02	0.02	0.03	-	-	-	-	0.03	0.216
Specimen 4	0.08	2.4	0.5	-	-	-	0.42	-	-	-	0.5	0.618

Table 1: Chemical composition of the specimens along with the carbon equivalent value.

3.2.2 Initialization

At the start of the simulation, various parameters have to be initialized. The table shows the initialized parameters. These initial values are taken as te input to run the simulation for the subsequent timestep.

Parameter	Variable	Value
Temperature	T	730 ^{0}C
Activation energy of migration	Q_g	141,500 J mol^{-1}
Pre-exponential factor	D_0	2.1× 10^{-5} m^{2}s^{-1}
Gas constant	R	8.314 J mol^{-1}K^{-1}
Dimension of each cell	L	1×10^-6 m

Table 2: Parameter values used during the diffusion process along with the its variables

3.2.3 Nucleation of austenite

In the present model the nucleation of austenite occurs at ferrite-pearlite interface. The pearlite is considered to be a uniform phase since the dimension of lamellar structure is in the order of 0.1 μm and the grains are in the order of 10 μm and this will increase the computational cost. For nucleation, cells which are in ferrite phase and have pearlite cells in their Moore's neighborhood are considered as nucleation site as per previously reported literature (Halder et al., 2014). This will restrict the nucleation cells only to the ferrite-pearlite interface. The favorable sites of nucleation are shown in Figure 3.7.

Figure 3.7: Illustration of preferred nucleation sites (cells with pink shade) for austenite (F-ferrirte, P- pearlite).

However, to compensate the structural error, the concentration of pearlite cells is taken as the eutectoid concentration. The eutectoid concentration of each of the sample is obtained from the ThermoCalc diagrams and is shown in **Figure 3.8**.

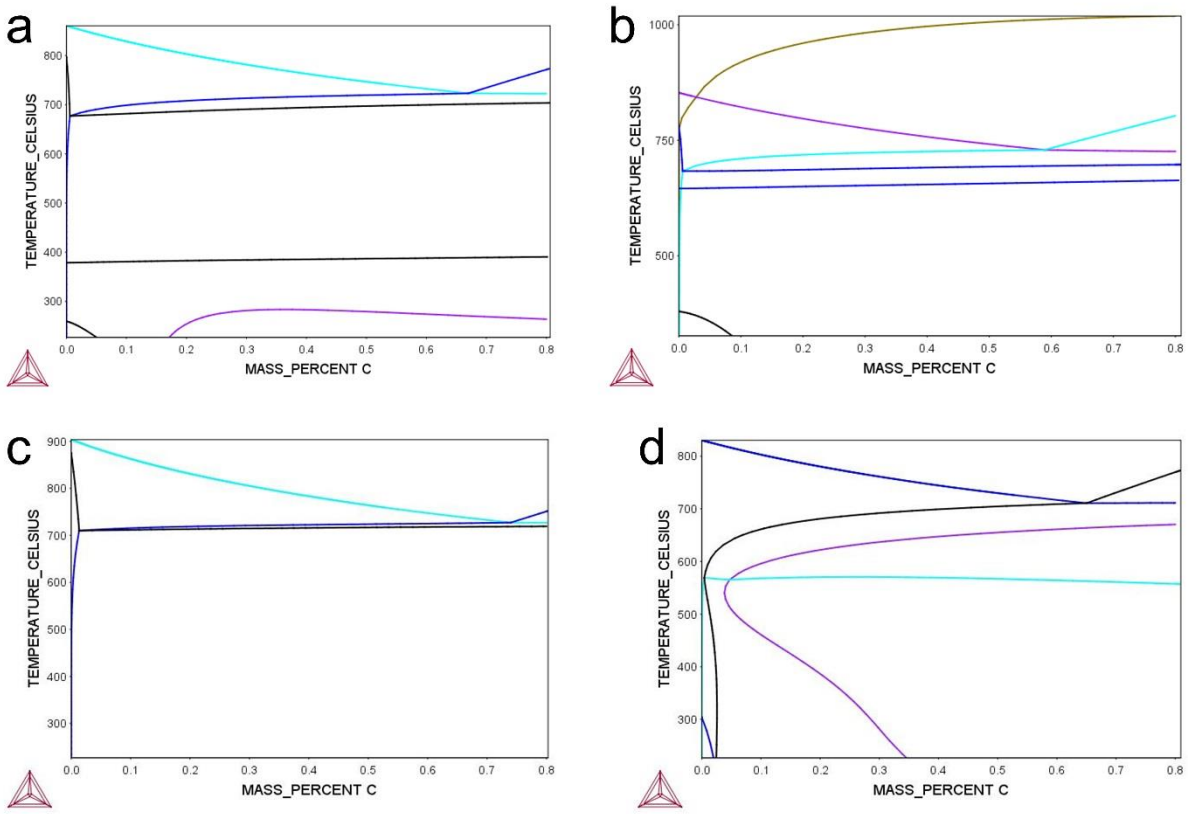

Figure 3.8: ThermoCalc Phase diagrams of dual phase steel of specimens: (a) Specimen 1, (b) Specimen 2, (c) Specimen 3, and (d) Specimen 4.

Nucleation occurs at a temperature above the A_{C1} line and the rate increases with increase in temperature. By literature, the number of austenite nuclei N is provided by the classical nucleation equation (Roosz et al., 1983):

$$N = \frac{1.378\ X\ 10^{-12}}{[(a^p)^2\sigma_0]^2} \exp\left(\frac{-25.38}{T-A_{C1}}\right) \frac{1}{mm^3 s} \qquad \textbf{Equation (4)}$$

Where T is the temperature in degree Celsius, $A_{C1}$is the eutectoid temperature in degree Celsius and a^p, σ_0 are the morphological parameters for pearlite. But since this present model considers pearlite as a uniform phase, the nucleation equation may fail in determining the number of nuclei at different temperatures. To overcome this drawback, a probabilistic algorithm has been developed to determine the number of favorable nuclei that transform into austenite. This algorithm counts the total number of favorable nucleation

site present in the microstructure model. It then assigns a finite number of nucleation sites for each temperature. Depending on the heating rate, some of these assigned nuclei change their state to austenite. High heating rate results in more nucleation whereas slower heating rate results in less nucleation. Hence, by this process the rate of nucleation changes as the temperature increases. Each cell which transforms into austenite nuclei takes a new state variable and a unique grain number but the carbon concentration is unchanged.

3.2.4 Growth process of austenite

Austenite growth is controlled by the carbon diffusion process. To maintain a constant overall carbon concentration, periodic boundary conditions are applied in the model.

Diffusion coefficient for the carbon diffusion is calculated using the following equation:

$$D_{\Psi} = D_0 \exp\left(\frac{-Q_g}{R\,T}\right) \qquad \textbf{Equation (5)}$$

where D_0- 2.1× 10^{-5} m^2s^{-1} (Kulakov et al., 2014) is the pre exponential factor, Q_g- 141,500 J mol^{-1} (Karacs and Roosz, 2008) is the activation energy of migration, R – 8.314 J $mol^{-1}K^{-1}$is the gas constant, T is the absolute temperature in K.

The transition rules for the model are established in such a way that it shows the actual kinetics of transformation. The first transition rule is for the pearlite dissolution. The pearlite cell transforms into austenite as soon as the carbon concentration of the pearlite cell is reduced below the eutectoid temperature. The second transition rule is for the transformation of ferrite into austenite. The concentration of each cell is checked with the equilibrium carbon concentration after each time step. When carbon concentration of austenite cell exceeds the equilibrium carbon concentration at that temperature then the neighbor ferrite cells transform into austenite.

To obtain realistic transformation kinetics, the equilibrium carbon concentration (Ac3 line) curve is divided into line segments in different temperature range and linearly fit. The equilibrium carbon concentration is calculated by using equation 5. Table 2 provides the values for $C_{\gamma\alpha 0}^{Ac3}$ and $C_{\gamma\alpha 1}^{Ac3}$ at different temperature range for the specimens by linear curve fitting the equilibrium carbon concentration line obtained from ThermoCalc software.

$$C_{\gamma\alpha}^{A_{c3}} = C_{\gamma\alpha 0}^{A_{c3}} + C_{\gamma\alpha 1}^{A_{c3}} T \qquad \textbf{Equation (6)}$$

Temperature Range		Specimen 1	Specimen 2	Specimen 3	Specimen 4
730 ^{0}C – 740 ^{0}C	$C_{\gamma\alpha 0}^{A_{c3}}$	6.0052	5.24362	5.53268	5.79362
	$C_{\gamma\alpha 1}^{A_{c3}}$	-0.00736	-0.00646	-0.0.658	-0.00727
740 ^{0}C – 780 ^{0}C	$C_{\gamma\alpha 0}^{A_{c3}}$	5.03996	4.38787	4.85085	4.62709
	$C_{\gamma\alpha 1}^{A_{c3}}$	-0.00606	-0.0053	-0.00568	-0.00569
780 ^{0}C – 800 ^{0}C	$C_{\gamma\alpha 0}^{A_{c3}}$	4.08956	3.77083	4.03145	3.77593
	$C_{\gamma\alpha 1}^{A_{c3}}$	-0.00484	-0.0045	-0.00462	-0.0046
800^{0}C – 820 ^{0}C	$C_{\gamma\alpha 0}^{A_{c3}}$	3.52916	3.23461	3.51962	3.1300
	$C_{\gamma\alpha 1}^{A_{c3}}$	-0.00413	-0.00382	-0.00399	-0.00379
820^{0}C – 880 ^{0}C	$C_{\gamma\alpha 0}^{A_{c3}}$	2.8849	2.67938	2.94599	3.00946
	$C_{\gamma\alpha 1}^{A_{c3}}$	-0.00335	-0.00315	-0.00329	-0.00364

Table 3: Values for $C_{\gamma\alpha 0}^{A_{c3}} and C_{\gamma\alpha 1}^{A_{c3}}$ at different temperature range for the specimens by linear curve fitting the equilibrium carbon concentration line obtained from ThermoCalc software.

The temperature for the next time step is calculated according to the following equation:

$$T^{t+1} = T^{t} + \Delta t\, H \qquad \textbf{Equation (7)}$$

Where H represents the heating rate and is equal to 3 ^{0}C/s, Δt is the time interval.

3.3 Algorithm

3.3.1 Carbon diffusion

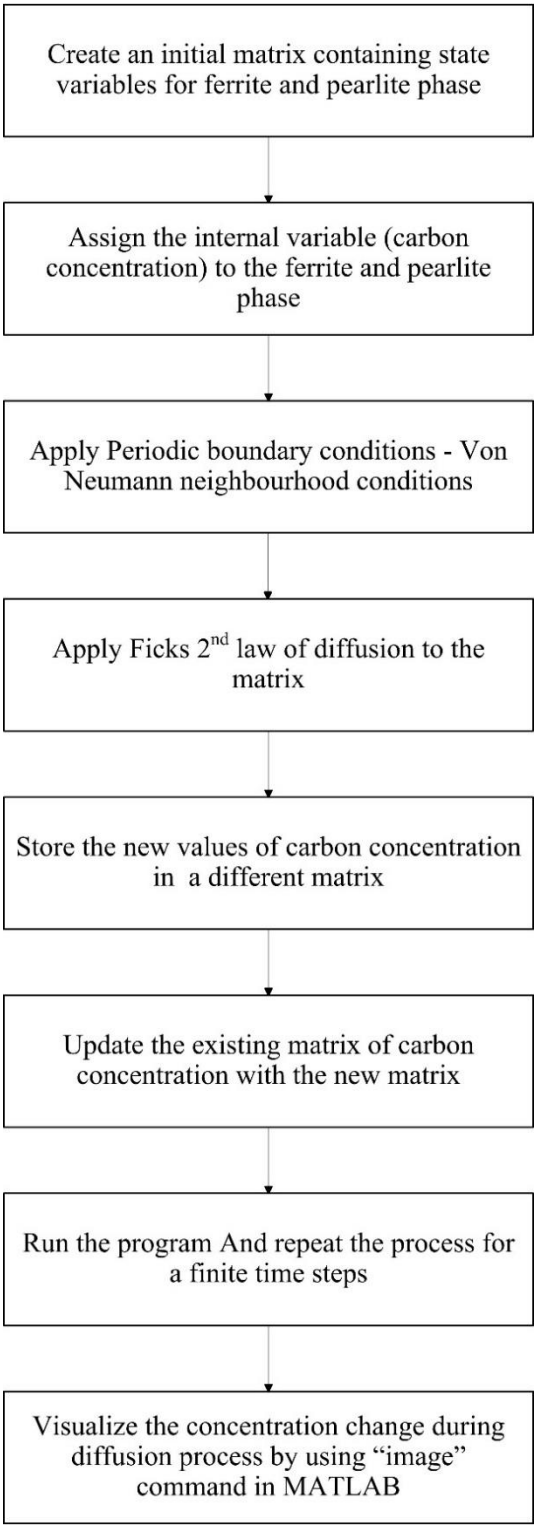

Figure 3.9: Flow chart showing the steps for carbon diffusion process during the simulation.

3.3.2 Grain growth

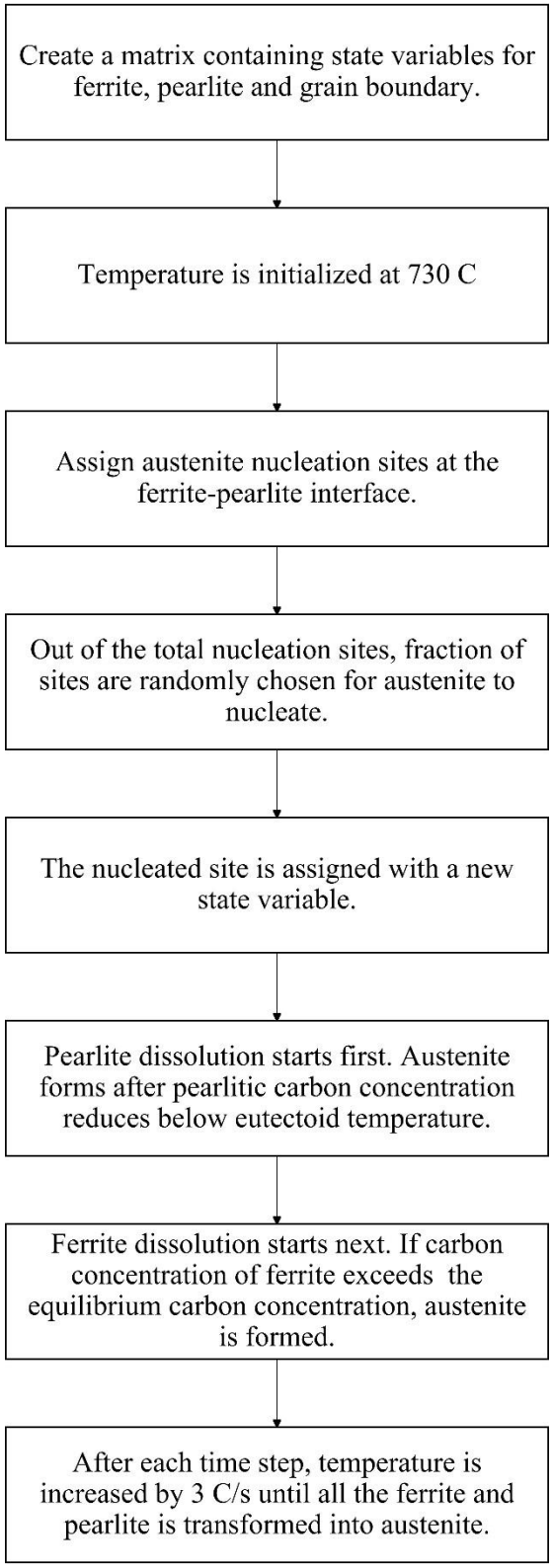

Figure 3.10: Flow chart showing the steps for austenitic growth process during the simulation.

Chapter 4

Results and Discussion

The representative initial microstructure and final transformed microstructure after simulated inter-critical heating up till 850ºC for specimen 1 is shown in Figure 4.1 (a) and Figure 4.1 (b) respectively**.** Final microstructure contains austenite grains, as all the pearlite and ferrite grains are transformed into austenite after the inter-critical heating.

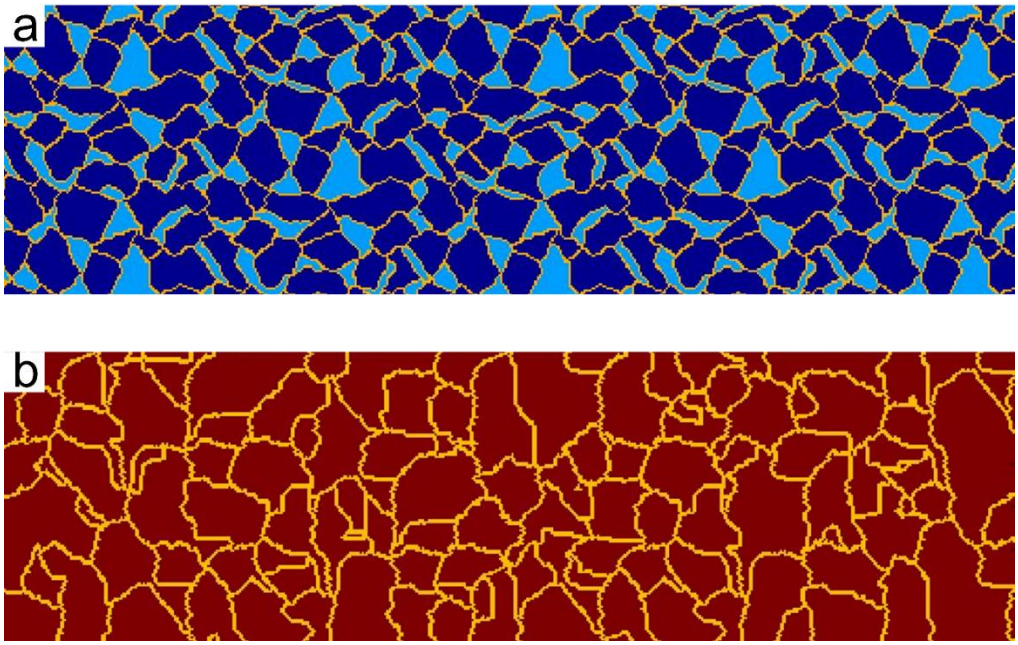

Figure 4.1: (a) Initial microstructure as input for the simulation. (b) Final microstructure after transformation. (P- Pearlite, α- Ferrite, ɣ- Austenite)

The microstructure evolution of austenite along with the diffusion of carbon at different temperature during heating is presented in Figure 4.2. The pearlite dissolution starts 730ºC temperatures for all the specimens, which is evident from the representative microstructure of specimen 1 given in Figure 4.2 (a). As the temperature increases, more and more pearlite is consumed for austenite transformation as per Figure 4.2. The carbon diffusion increases with the increasing temperature which results in diffusion of carbon from super saturated

austenite and consequently concentration of carbon in austenite reaches to equilibrium state and the growth of austenite becomes steady. The complete austenite formation at 850ºC is evident in Figure 4.2 (d).

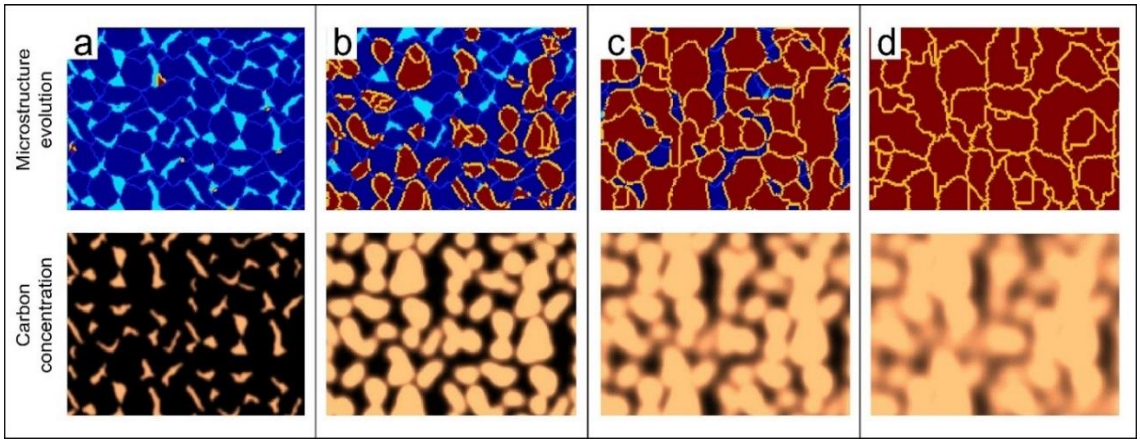

Figure 4.2: Microstructure evolution along with carbon diffusion process during phase transformation at different temperatures: (a) 730 ºC, (b) 770 ºC (c) 810 ºC, (d) 850 ºC.

The calculated austenite volume fraction and the experimental value obtained from literature (Halder et al., 2014) at different temperature for specimen is plotted in Figure 4.3. The results obtained from the present simulation using CA method are found in a good agreement with the experiment.

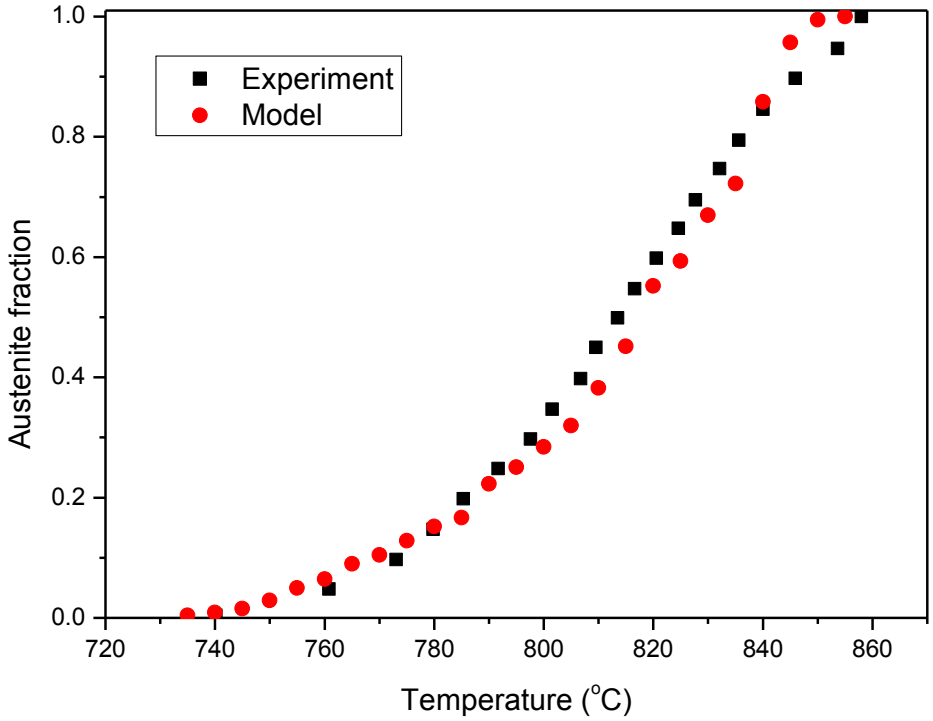

Figure 4.3: Experimental validation of the simulated model for 3 °C/s heating rate.

It is obvious from Figure 4.3 that the model can predict appropriately the austenite volume fraction after efficiently simulating the phase transformation kinetics for inter-critical heating of DP steel.

Austenite volume fraction vs temperature for all four specimens is also plotted in separate figure to evaluate the effect of carbon equivalent on the volume fraction of austenite formed during inter-critical heating as shown in Figure 4.4 (a). It is observed that complete transformation into austenite is completed at 890°C for specimen 4 which has lowest carbon equivalent. On the other hand, austenite grows fastest and complete transformation occurs before 825 °C for specimen 3, which possess highest carbon equivalent content value. The pearlite fractions at different temperature for all four speimens are presented in Figure 4.4 (b). The complete pearlite dissolution is observed for all the specimens. In case of specimen having higher carbon equivalent, complete pearlite dissolution takes place at faster rate and lower temperature compared to the specimen having lower carbon equivalent. Therefore, it

is inferred that the presence of carbon and alloying elements contributing in increment of carbon equivalent helps in faster formation of austenite.

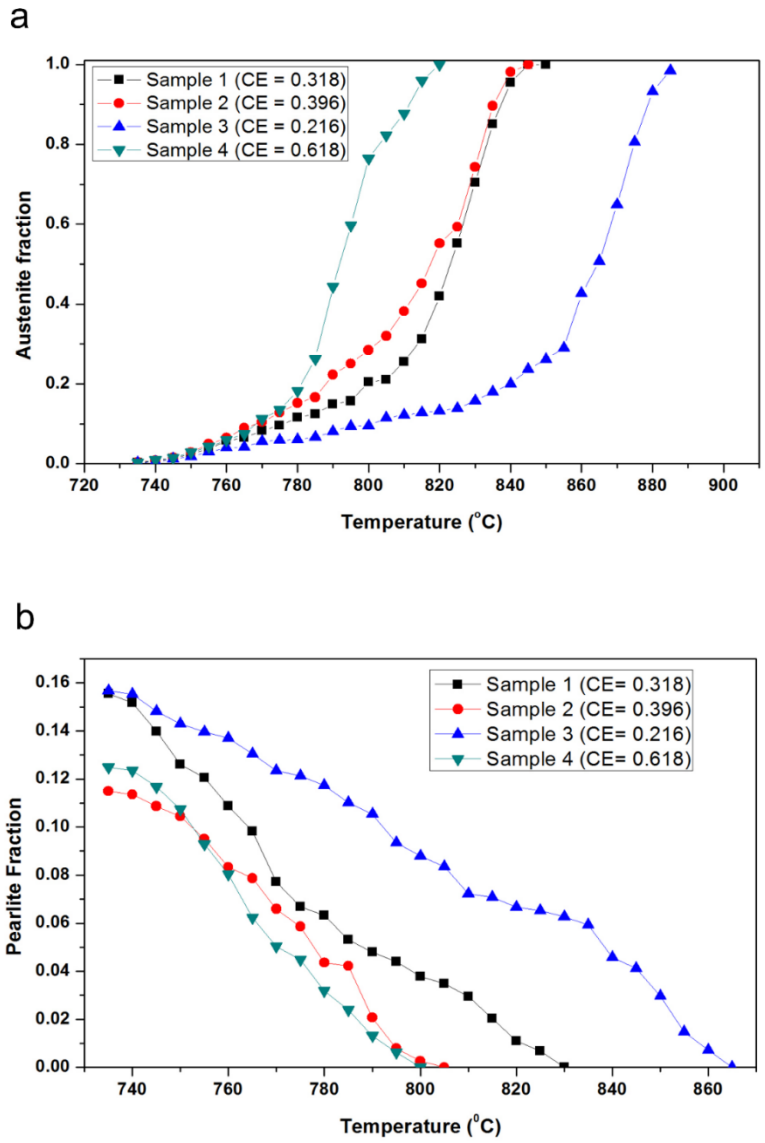

Figure 4.4: Graph showing (a) the austenite fraction at different temperature for the specimens, (b) the pearlite fraction at different temperature for the specimens.

Chapter 5

Conclusion

A model for phase transformation during inter-critical heating of DP steel based on cellular automata method is designed and developed to predict microstructure and formation of austenite. The present study shows the capability of cellular automata based model for efficient simulation of phase transformation for DP steel. The model considers pearlite dissolution, ferrite transformation and austenite grain growth. This study shows that the carbon equivalent value is important for austenite transformation during inter-critical heating of DP steels. Complete austenite transformation occurs faster for DP steels having higher carbon equivalent. The output of this predictive model is found to be in good agreement with literature reported experimental results. This model can be extended and updated for identification and subsequent optimization of controlling parameters of phase transformation relevant to steel.

Bibliography

Al-Abbasi, F. M., & Nemes, J. A. (2003). Micromechanical modeling of dual phase steels. International Journal of Mechanical Sciences, 45(9), 1449-1465.

Rashid, M. S. (1981). Dual phase steels. Annual Review of Materials Science, 11(1), 245-266.

Sarwar, M., & Priestner, R. (1996). Influence of ferrite-martensite microstructural morphology on tensile properties of dual-phase steel. Journal of Materials Science, 31(8), 2091-2095.

Rocha, R. O., Melo, T. M. F., Pereloma, E. V., & Santos, D. B. (2005). Microstructural evolution at the initial stages of continuous annealing of cold rolled dual-phase steel. Materials Science and Engineering: A, 391(1), 296-304.

Allam, T., & Abbas, M. (2015). Mechanical Properties, Formability, and Corrosion Behavior of Dual Phase Weathering Steels Developed by an Inter-Critical Annealing Treatment. Steel research international, 86(3), 231-240.

Movahed, P., Kolahgar, S., Marashi, S. P. H., Pouranvari, M., & Parvin, N. (2009). The effect of intercritical heat treatment temperature on the tensile properties and work hardening behavior of ferrite–martensite dual phase steel sheets. Materials Science and Engineering: A, 518(1), 1-6.

Hofmann, H., Mattissen, D., & Schaumann, T. W. (2009). Advanced cold rolled steels for automotive applications. Steel Research International, 80(1), 22-28.

Matlock, D. K., Speer, J. G., De Moor, E., & Gibbs, P. J. (2012). Recent developments in advanced high strength sheet steels for automotive applications: an overview. Jestech, 15(1), 1-12.

Maleque, M. A., Poon, Y. M., & Masjuki, H. H. (2004). The effect of intercritical heat treatment on the mechanical properties of AISI 3115 steel.Journal of materials processing technology, 153, 482-487.

Erdogan, M. (2003). Effect of austenite dispersion on phase transformation in dual phase steel. Scripta Materialia, 48(5), 501-506.

Zhang, L., Zhang, C. B., Wang, Y. M., Wang, S. Q., & Ye, H. Q. (2003). A cellular automaton investigation of the transformation from austenite to ferrite during continuous cooling. Acta Materialia, 51(18), 5519-5527.

Pandi, R., & Yue, S. (1994). Dynamic transformation of austenite to ferrite in low carbon steel. ISIJ international, 34(3), 270-279.

Ricks, R. A., Southwick, P. D., & Howell, P. R. (1981). The effect of chromium and nickel on the γ→ α phase transformation in steels and iron-base alloys. Journal of Microscopy, 124(1), 23-35.

Cao, J. C., Liu, Q. Y., Yong, Q. L., & Sun, X. J. (2007). Effect of niobium on isothermal transformation of austenite to ferrite in HSLA low-carbon steel. Journal of Iron and Steel Research, International, 14(3), 52-56.

Huang, J., Poole, W. J., & Militzer, M. (2004). Austenite formation during intercritical annealing. Metallurgical and Materials Transactions A, 35(11), 3363-3375.

Schemmann, L., Zaefferer, S., Raabe, D., Friedel, F., & Mattissen, D. (2015). Alloying effects on microstructure formation of dual phase steels.Acta Materialia, 95, 386-398.

Girina, O., Fonstein, N., Panahi, D., Bhattacharya, D., & Jansto, S. (2015). The Influence of Mo, Cr and B Alloying on Phase Transformation and Mechanical Properties in Nb Added High Strength Dual Phase Steels. InHSLA Steels 2015, Microalloying 2015 & Offshore Engineering Steels 2015: Conference Proceedings (pp. 237-245). John Wiley & Sons, Inc.

Speich, G. R., Demarest, V. A., & Miller, R. L. (1981). Formation of austenite during intercritical annealing of dual-phase steels. Metallurgical Transactions A, 12(8), 1419-1428.

Takahama, Y., Santofimia, M. J., Mecozzi, M. G., Zhao, L., & Sietsma, J. (2012). Phase field simulation of the carbon redistribution during the quenching and partitioning process in a low-carbon steel. Acta Materialia, 60 (6), 2916-2926.

Li, H., Gai, K., He, L., Zhang, C., Cui, H., & Li, M. (2016). Non-isothermal phase-transformation kinetics model for evaluating the austenization of 55CrMo steel based on Johnson–Mehl–Avrami equation. Materials & Design, 92, 731-741.

Han, F., Chen, R., Yang, C., Li, X., & Wang, D. (2016, February). Cellular Automata Simulation on Dynamic Recrystallization of TA16 Alloy during Hot Deformation. In Materials Science Forum (Vol. 849).

Lin, Y. C., Liu, Y. X., Chen, M. S., Huang, M. H., Ma, X., & Long, Z. L. (2016). Study of static recrystallization behavior in hot deformed Ni-based superalloy using cellular automaton model. Materials & Design, 99, 107-114.

Kim, N. J., & Thomas, G. (1981). Effects of morphology on the mechanical behavior of a dual phase Fe/2Si/0.1 C steel. Metallurgical Transactions A, 12(3), 483-489.

Todinov, M. T. (2000). On some limitations of the Johnson–Mehl–Avrami–Kolmogorov equation. Acta Materialia, 48(17), 4217-4224.

Kulakov, M., Poole, W. J., & Militzer, M. (2014). A Microstructure Evolution Model for Intercritical Annealing of a Low-carbon Dual-phase Steel. ISIJ International, 54(11), 2627-2636.

Pietrzyk, M., Kuziak, R., Radwański, K., & Szeliga, D. (2014). Physical and numerical simulation of the continuous annealing of DP steel strips. Steel research international, 85(1), 99-111.

Zhu, B., & Militzer, M. (2015). Phase-field modeling for intercritical annealing of a dual-phase steel. Metallurgical and Materials Transactions A, 46(3), 1073-1084.

Zhu, G., Kang, Y., Lu, C., & Li, S. (2014). Microstructure Evolution of Cold-Rolled Dual Phase Steel Simulated by Cellular Automata. Steel research international, 85(6), 1035-1046.

Bos, C., Mecozzi, M. G., & Sietsma, J. (2010). A microstructure model for recrystallisation and phase transformation during the dual-phase steel annealing cycle. Computational Materials Science, 48(3), 692-699.

Pietrzyk, M., Madej, L., Rauch, L., & Szeliga, D. (2015). Computational Materials Engineering: Achieving High Accuracy and Efficiency in Metals Processing Simulations. Butterworth-Heinemann.

Madej, L., Sieradzki, L., Sitko, M., Perzynski, K., Radwanski, K., & Kuziak, R. (2013). Multi scale cellular automata and finite element based model for cold deformation and annealing of a ferritic–pearlitic microstructure. Computational Materials Science, 77, 172-181.

Han, F., Tang, B., Kou, H., Cheng, L., Li, J., & Feng, Y. (2014). Static recrystallization simulations by coupling cellular automata and crystal plasticity finite element method using a physically based model for nucleation. Journal of Materials Science, 49(8), 3253-3267.

Mecozzi, M. G., Bos, C., & Sietsma, J. (2011, June). 3D Cellular Automata Modelling of Solid–state Transformations Relevant in Low–alloy Steel Production. In Solid State Phenomena (Vol. 172, pp. 1140-1145).

Halder, C., Madej, L., & Pietrzyk, M. (2014). Discrete micro-scale cellular automata model for modelling phase transformation during heating of dual phase steels. Archives of civil and mechanical engineering, 14(1), 96-103.

Zheng, C., & Raabe, D. (2013). Interaction between recrystallization and phase transformation during intercritical annealing in a cold-rolled dual-phase steel: A cellular automaton model. Acta Materialia, 61(14), 5504-5517.

Ahmad, E., Karim, F., Saeed, K., Manzoor, T., & Zahid, G. H. (2014). Effect of cold rolling and annealing on the grain refinement of low alloy steel. In IOP Conference Series: Materials Science and Engineering (Vol. 60, No. 1, p. 012029). IOP Publishing.

Reed-Hill, R. E., & Abbaschian, R. (1973). Physical metallurgy principles.

Speich, G. R., Demarest, V. A., & Miller, R. L. (1981). Formation of austenite during intercritical annealing of dual-phase steels. Metallurgical Transactions A, 12(8), 1419-1428.

Maalekian M, Institut für Werkstoffkunde. Technische Universität Graz 36 (2007).

Kasuya, T., & Yurioka, N. (1993). Carbon equivalent and multiplying factor for hardenability of steel. WELDING JOURNAL-NEW YORK-, 72, 263-s.

Roosz, A., Gacsi, Z., & Fuchs, E. G. (1983). Isothermal formation of austenite in eutectoid plain carbon steel. Acta Metallurgica, 31(4), 509-517.

Karacs, G., & Roósz, A. (2008, September). A Two-Dimensional Cellular Automaton Simulation for the Description of the Austenitization in Hypoeutectoid and Eutectoid Fe-C Steels. In Materials Science Forum (Vol. 589, pp. 317-322).

Dissemination

Articles published

Reddy, K. V., Halder, C., & Pal, S. Influence of Carbon Equivalent Content on Phase Transformation During Inter-critical Heating of Dual Phase Steels Using Discrete Micro-scale Cellular Automata Model. Transactions of the Indian Institute of Metals, 1-7 (**Accepted**).